Article:
Yang, L, Fan, P, McLernon, D et al. (2023) Data-aided Active User Detection with False Alarm Correction in Grant-Free Transmission. IEEE Wireless Communications Letters, 12 (1). pp. 143-147. ISSN: 2162-2337

https://doi.org/10.1109/LWC.2022.3219414

Data-aided Active User Detection with False Alarm Correction in Grant-Free Transmission

Linjie Yang, *Student Member, IEEE*, Pingzhi Fan, *Fellow, IEEE*, Des McLernon, *Member, IEEE*, Li Zhang *Senior Member, IEEE*

***Abstract*—In most existing grant-free (GF) studies, the two key tasks, namely active user detection (AUD) and payload data decoding, are handled separately. In this paper, a two-step data-aided AUD scheme is proposed, namely the initial AUD step and the false alarm correction step respectively. To implement the initial AUD step, an embedded low-density-signature (LDS) based preamble pool is constructed. In addition, two message passing algorithm (MPA) based initial estimators are developed. In the false alarm correction step, a redundant factor graph is constructed based on the initial active user set, on which MPA is employed for data decoding. The remaining false detected inactive users will be further detected by the false alarm corrector with the aid of decoded data symbols. Simulation results reveal that both the data decoding performance and the AUD performance are significantly enhanced by more than 1.5 dB at the target accuracy of 10^{-3} compared with the traditional compressed sensing (CS) based counterparts.**

***Index Terms*—Grant free, False alarm correction, MPA**

I. Introduction

Massive machine-type communication (mMTC) is one of the most popular services in fifth-generation (5G) mobile communication systems. Since conventional orthogonal multiple access (OMA) cannot meet the explosive demand due to the limited orthogonal resources, non-orthogonal multiple access (NOMA) technologies are advocated to support the massive connectivity. Among the many available NOMA schemes, low-density-signature orthogonal frequency division multiplexing (LDS-OFDM) [1] is one of the most generic solutions in code domain. In an LDS-OFDM system, the message passing algorithm (MPA) with near-optimal performance is employed to cancel interference among multiple users. Benefiting from the LDS structure, the complexity of the MPA algorithm becomes affordable. However, the MPA algorithm is implemented based on the assumption that each user's activity information is perfectly known at the base station (BS). However, in massive IoT networks, this assumption is impractical.

Now in 5G New Radio, the approval proposed to reduce latency is grant-free(GF) random access. This means channel resources can be accessed without being arranged through a handshaking process. To realize the GF requirement of LDS-OFDM system, there are two mainstream solutions widely studied. Firstly, a framework referred to as compressed sensing based MPA (CS-MPA) detector is proposed where active users will transmit their specific non-orthogonal preamble with length L_p before their data transmission begins [2], [3]. By leveraging users' activity sparsity, the active user detection (AUD) task is formulated as a standard CS problem and solved by the existing CS recovery algorithms efficiently, e.g. orthogonal matching pursuit (OMP) [2], dynamic compressed sensing (DCS) [3], and approximate message passing algorithm (AMP) [4] etc. Then, MPA is performed to reliably detect the transmitted symbols of the active users. On the other hand, some researchers propose to add an extended zero constellation point into the conventional LDS constellation alphabet [5]. The key idea is that one can recognize the activity states of users through their decoded symbols, i.e. if the detected zero symbols in a user's packet is large enough, this user is considered as inactive.

However, in a CS-MPA detector, the AUD and data payload decoding are normally handled separately. The feasibility that error correction with the aid of decoded data symbols provides additional mechanism for performance improvement is ignored [6]. In [5], MPA is directly employed to decode data symbols of all potential users, at the absence of activity state information of potential users in the cell. But, the complexity of this approach would become prohibitive upon the increase of the potential user number.

Based on the above discussion, Our main contributions in this paper are summarized as follows.

- Firstly, a data-aided two-step AUD scheme is proposed. In step 1, an initial active user set which contains a small number of false alarms is estimated by the initial estimator from the received preamble signal. In step 2, these false alarms are further corrected by the designed false alarm corrector.
- Secondly, to estimate an initial active user set, an embedded LDS based preamble pool is firstly constructed. Then, an MPA based initial estimator is presented. To reduce the complexity of the MPA detector, a traffic load aided MPA (TL-MPA) based detector is further proposed.
- Finally, based on the fact that if a user is inactive, the number of detected zero symbols should be large, a false alarm corrector based on multiple zero symbol detection is implemented in the data decoding process to peel off the remaining false alarms in the initial active user set.

This work was supported by NSFC Project No.62020106001 and No.61731017, and 111 Project No.111-2-14.

Linjie Yang and Pingzhi Fan are with the Information Coding & Transmission Key Lab of Sichuan Province, CSNMT Int. Coop. Res. Centre (MoST), Southwest Jiaotong University, Chengdu 611756, China (e-mail: yanglinjie@my.swjtu.edu.cn, p.fan@ieee.org).

Des McLernon and Li Zhang are with the School of Electronic and Electrical Engineering, University of Leeds, Leeds LS2 9JT, UK (e-mail: D.C.McLernon@leeds.ac.uk, L.X.Zhang@leeds.ac.uk)

The rest of the paper is orgnised as follows. System model is introduced in Section II. The construction method of embedded LDS based user preamble and two MPA based initial estimators are depicted in Section III. In Section IV, the proposed false alarm corrector is described. Complexity analysis is provided in Section V. Simulation results are presented in Section VI. Finally, the paper is concluded in Section VII.

II. System model

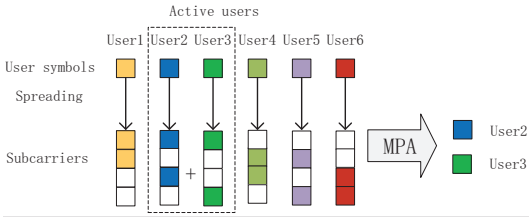

Figure 1. Graphic representation of the GF LDS-OFDM, where potential user number $N = 6$, active user number $N_a = 2$, sub-carriers number $L_s = 4$.

An up-link scenario of a single IoT cell with N IoT devices each of which is assigned a user-specific preamble, is considered. Only N_a users are active at any given time point. The sparsity λ is defined as $\lambda = \frac{N_a}{N}$. Meanwhile, only a single antenna is considered at both the user side and base station (BS) for low-cost IoT. Moreover, perfect symbol-wise synchronization is assumed.

The whole transmission period contains two stages, namely the preamble transmission stage and the data transmission stage. In the preamble transmission stage, for user $u, 1 \leq u \leq N$, once it becomes active, its activity state changes to $a_u = 1$ from $a_u = 0$. Then, its user-specific preamble $\mathbf{s}_u$ with length L_p is transmitted to the BS in a GF manner [4]. The construction of a users' preamble pool will be elaborated later in Section III. After that, its data transmission stage begins. Firstly, its data packet $\mathbf{x}_u = [x_u[1], x_u[2], \cdots, x_u[K]] \in \mathbb{C}^{K\times 1}$ is prepared. The k^{th} data symbol $x_u[k], 1 \leq k \leq K$ is selected from the alphabet $\mathcal{X}_u = \mathcal{X} \cup \{0\}$. The original alphabet $\mathcal{X}$ is generated according to [7] where each standard $M-$ary phase shift keying (PSK) symbol is multiplied by a user-specific complex coefficient. The cardinality of the final alphabet is $M + 1$. Then, $\mathbf{x}_u$ is modulated onto a user specific signature sequence $\mathbf{c}_u$ with length L_s. All active users' signals are superposed and propagated simultaneously over L_s sub-carriers. In this paper, the signature sequence $\mathbf{c}_u, 1 \leq u \leq N$ is selected from the columns of the parity check matrix of a regular low-density-parity-check (LDPC) code. For the example in Figure. 1, the LDS signature matrix $\mathbf{C}_{4,6} = [\mathbf{c}_1, \mathbf{c}_2, \cdots, \mathbf{c}_6]$ is given by

$$\mathbf{C}_{4,6} = \begin{bmatrix} 1 & 1 & 1 & 0 & 0 & 0 \\ 1 & 0 & 0 & 1 & 1 & 0 \\ 0 & 1 & 0 & 1 & 0 & 1 \\ 0 & 0 & 1 & 0 & 1 & 1 \end{bmatrix}. \tag{1}$$

At the receiver side, the received signal of users' preamble can be modeled as

$$\mathbf{y}_p = \sum_{u=1}^{N} a_u(\mathbf{h}_u^p \circ \mathbf{s}_u) + \mathbf{n}_p. \tag{2}$$

where '$\circ$' denotes Hadamard product. The received signal of $k^{th}, 1 \leq k \leq K$ data symbol on the l_s^{th} sub-carrier is modeled as

$$\mathbf{y}[l_s, k] = \sum_{u=1}^{N} a_u \mathbf{h}_u^d[l_s, k]\mathbf{c}_u[l_s]\mathbf{x}_u[k] + \mathbf{n}_d[l_s, k], \tag{3}$$

where $\mathbf{c}_u[l_s], 1 \leq l_s \leq L_s$ denotes the l_s^{th} component of $\mathbf{c}_u$. Here, $\mathbf{h}_u^p$ and $\mathbf{h}_u^d$ denote the complex channel coefficient between user u and the BS in the preamble transmission period and data transmission period respectively, and are sampled independently from the distribution $\mathcal{CN}(0, 1)$ [2], [3]. Also, $\mathbf{n}_p \in \mathbb{C}^{L_s\times 1}$ and $\mathbf{n}_d \in \mathbb{C}^{L_s\times K}$ represent background noise which obeys i.i.d. Gaussian distribution $\mathcal{CN}(0, \sigma^2\mathbf{I})$. Additionally, as stated in [2], [3], the preamble length equals the sub-carrier number, i.e. $L_s = L_p$ in this paper.

III. Initial Active Uset Set Detection

A. Embedded LDS based User Preamble Construction

To obtain the initial active user set, which is also referred to as the super-set $\hat{\mathcal{U}}_{ac}^I$ (i.e. $\mathcal{U}_{ac} \subset \hat{\mathcal{U}}_{ac}^I$ [8]), only a test on each sub-carrier is required [9]. If there is no user transmitting data on the l_s^{th} sub-carrier, the l_s sub-carrier is idle and the outcome of the test is $\mathbf{Y}_t[l_s] = 0$. Otherwise, the l_s sub-carrier is busy and $\mathbf{Y}_t[l_s] = 1$. Then, based on $\mathbf{Y}_t$, $\hat{\mathcal{U}}_{ac}^I$ can be efficiently estimated with a cover decoder by directly removing the inactive users, i.e. $\{u|\mathbf{C}[l_s, u] = 1, Y_t[l_s] = 0\}$ [9].

Informed by [9], in our case, the target of the user preamble $\mathbf{s}_u, 1 \leq u \leq N$ is converted to convey the non-zero elements' positions in the signature sequence $\mathbf{c}_u$, rather than conveying its identity directly. To this end, we first generate a Zad-off Chu (ZC) sequence $\mathbf{z}_r[n]$ and its L_s-1 cyclic-shifting versions $\mathbf{z}_r[n + 1], \cdots, \mathbf{z}_r[n + L_s - 1]$ to form a ZC sequence set, $\{\mathbf{z}_r[n], \mathbf{z}_r[n+1] \cdots \mathbf{z}_r[n+L_s-1]\}$. $\mathbf{z}_r[n] = \exp[-j\pi rn(n+1)/L_s], n = 0, 1, \cdots, L_s - 1$ denote a ZC sequence with root number r [10]. Then, for user $u, 1 \leq u \leq N$, each l_s^{th} ZC sequence is selected once $\mathbf{c}_u[l_s] = 1$. Finally, combine these selected ZC sequences to form the preamble of user u, $\mathbf{s}_u$. The embedded LDS based preamble construction is summarized as

$$\mathbf{s}_u = \frac{1}{\sqrt{w_c}} \sum_{l_s=1}^{L_s} \mathbf{c}_u[l_s]\mathbf{z}_r[n + l_s - 1]. \tag{4}$$

Lastly, the column weight w_c of $\mathbf{C}$ is introduced to normalize the unit power of the constructed user preamble.

B. MPA based initial estimator

At the receiver, as reported in [11], the channel variation is very small in short packet transmission scenarios of mMTC. As a result, the elements of $\mathbf{h}_u^p$ in (2) may reasonably be considered constant over the preamble duration. i.e. $\mathbf{h}_u^p[l] \approx h_u^p, 1 \leq l \leq L_p$, which significantly simplifies the design of the initial estimator. To be more concrete, the correlation value $\mathbf{R}[l_s], 1 \leq l_s \leq L_s$ between the preamble received signal $\mathbf{y}_p$

and the aforementioned L_s reference ZC sequences $\mathbf{z}_r[n+l_s], 0 \le l_s \le L_s-1$ in Section III is first calculated.

$$\mathbf{R}[l_s] = \frac{\sqrt{w_c}}{N_{zc}} | \sum_{n=0}^{N_{zc}-1} \mathbf{y}_p \mathbf{z}_r^{\star}[n+l_s]|, \tag{5}$$

where $(\cdot)^{\star}$ is the complex conjugate operator. As discussed in Section III.A, we can simply estimate $\mathbf{Y}_t[l_s], 1 \le l_s \le L_s$ based on $\mathbf{R}[l_s], 1 \le l_s \le L_s$, and then, obtain $\hat{\mathcal{U}}_{ac}^I$ by a cover decoder in [9].

However, a cover decoder will only make a hard decision according to the estimation of $\mathbf{Y}_t[l_s], 1 \le l_s \le L_s$, which is sensitive to the background noise. To improve the robustness of the initial estimator, an MPA based detector is proposed. Based on $\hat{\mathcal{U}}_{ac}^I$, a redundant factor graph $\mathcal{G}(\hat{\mathcal{U}}_{ac}^I)$ can be constructed by regarding the sub-carriers as the check nodes and users in $\hat{\mathcal{U}}_{ac}^I$ as the variable nodes. Define $\mathcal{N}(u)$ as the neighbor nodes connected to the u^{th} variable node. $\mathcal{N}(u)\backslash l_s$ means excluding the l_s^{th} check node from $\mathcal{N}(u)$. $\mathcal{N}(l_s)$ denotes the neighbor nodes connected to the l_s^{th} check node. $\mathcal{N}(l_s)\backslash u$ denotes excluding u^{th} variable node from $\mathcal{N}(l_s)$. According to [10], the values of $\mathbf{R}$ defined in (5) obey a Rice distribution, i.e. $\mathbf{R}[l_s] \sim \mathrm{Rice}(\sum_{u' \in \mathcal{N}(l_s)} a_{u'} h_{u'}^p, \frac{\sigma}{\sqrt{2N_{zc}}})$. We denote the probability density function of the Rice distribution as

$$\mathrm{Rice}(x|A,\sigma) = \frac{x}{\sigma^2} \exp(-\frac{x^2+A^2}{2\sigma^2}) I_0(\frac{xA}{\sigma^2}), \tag{6}$$

where $I_0(\cdot)$ is the modified Bessel function of the first kind with the order zero. The rules of the proposed MPA detector in the i^{th} iteration are given by

$$\begin{aligned} E_{l_s \to u}^{(i)}(a_u) = \mathcal{R} \sum_{\substack{u' \in \mathcal{N}(l_s)\backslash u \\ a_{u'} \in \{0,1\}}} \mathrm{Rice}(\mathbf{R}[l_s] \mid a_u h_u^p + \sum_{u' \in \mathcal{N}(l_s)\backslash u} a_{u'} h_{u'}^p, \\ \sigma/\sqrt{2N_{zc}}) \cdot \prod_{u' \in \mathcal{N}(l_s)\backslash u} E_{u' \to l_s}^{(i-1)}(a_{u'}), \end{aligned} \tag{7}$$

$$E_{u \to l_s}^{(i)}(a_u) = \prod_{l_s' \in \mathcal{N}(u)\backslash l_s} E_{l_s' \to u}^{(i-1)}(a_u), \tag{8}$$

where $E_{l_s \to u}^{(i)}(a_u)$ denotes the extrinsic information passed from the l_s^{th} check node to the u^{th} variable node in the i^{th} iteration. $E_{u \to l_s}^{(i)}(a_u)$ denotes the extrinsic information passed from the u^{th} variable node to the l_s^{th} check node in the i^{th} iteration. Then constant $\mathcal{R}$ is chosen such that $E_{l_s \to u}^{(i)}(a_u = 0) + E_{l_s \to u}^{(i)}(a_u = 1) = 1$. The MPA based detector is initialized by $E_{u \to l_s}^{(0)}(a_u = 1) = \lambda$ and $E_{u \to l_s}^{(0)}(a_u = 0) = 1 - \lambda$. Then, the *a posterior* probability whether user u is active is computed as $E(a_u) = \prod_{l_s' \in \mathcal{N}(u)} E_{l_s' \to u}^{(i)}(a_u)$.

Note that in our scheme, the missing detection should be avoided as much as possible [9]. Hence, the decision rule of the proposed MPA based detector is

$$\hat{a}_u = \begin{cases} 0, & E(a_u = 0) > 0.99 \\ 1, & \text{otherwise} \end{cases} \tag{9}$$

C. Traffic load aided MPA (TL-MPA) based initial estimator

The search space of the proposed MPA based detector in (8) is in the order of $\mathcal{O}(2^{w_r})$. w_r denotes the row weight of $\mathbf{C}$. The search space can be further reduced. Now, the traffic load of l_s^{th} sub-carrier $\mathbf{Y}_l[l_s]$ can be estimated as

$$\begin{aligned} \mathbf{a}_{l_s} &= \underset{u' \in \mathcal{N}(l_s)}{\arg\min} ||\mathbf{R}[l_s] - \mathbf{a}_{l_s}[u'] \mathbf{c}_{u'}[l_s] h_{u'}^p||_2^2 \\ \hat{\mathbf{Y}}_l[l_s] &= \sum_{u' \in \mathcal{N}(l_s)} \mathbf{a}_{l_s}[u'], \end{aligned} \tag{10}$$

where $\mathbf{a}_{l_s} = \{a_{u'} | u' \in \mathcal{N}(l_s)\}$ is the user activity vector of l_s^{th} sub-carrier. Meanwhile, $\mathbf{Y}_t$ can be estimated as

$$\hat{\mathbf{Y}}_t = \begin{cases} 0, & \hat{\mathbf{Y}}_l[l_s] = 0 \\ 1, & \text{otherwise} \end{cases} \tag{11}$$

In the detection process, we only search the possible combinations such that $\sum_{u' \in \mathcal{N}(l_s)} a_{u'} = \hat{\mathbf{Y}}_l[l_s]$ on the l_s^{th} sub-carrier. The search space is reduced to the order of $\mathcal{O}(\binom{\hat{\mathbf{Y}}_l[l_s]}{w_r})$ where $\binom{k}{n}$ denotes the number of combinations of n items taken k at a time. The decoding rules of TL-MPA are given by

$$E_{l_s \to u}^{(i)} = \log(\frac{p_{u,l_s}(a_u = 1)}{p_{u,l_s}(a_u = 0)}), \tag{12}$$

$$E_{u \to l_s}^{(i)} = \sum_{l_s' \in \mathcal{N}(u)\backslash l_s} E_{l_s' \to u}^{(i-1)}, \tag{13}$$

where

$$\begin{aligned} p_{u,l_s}(a_u) = \sum_{\substack{\sum a_{u'} = \hat{\mathbf{Y}}_l[l_s] \\ u' \in \mathcal{N}(l_s)}} \prod_{u' \in \mathcal{N}(l_s)\backslash u} (1 - p_{u',l_s}(a_{u'}))^{(1-a_{u'})} \\ \cdot (p_{u',l_s}(a_{u'}))^{a_{u'}} \exp(|\mathbf{R}[l_s] - \sum_{u' \in \mathcal{N}(l_s)} a_{u'} h_{u'}^p|^2), \end{aligned} \tag{14}$$

Particularly, $E_{l_s \to u}^{(i)} = -\infty$ if $\hat{\mathbf{Y}}_l[l_s] = 0$. The log-likelihood ratio (LLR) $\log(\frac{\mathrm{P}(a_u=1)}{\mathrm{P}(a_u=0)})$ is computed as $r_u = \sum_{l_s' \in \mathcal{N}(u)} E_{l_s' \to u}^{(i)}$. $E_{u \to l_s}^{(0)}$ is initialized as $\log(\frac{\lambda}{1-\lambda})$. Similar to the MPA based detector, the decision rule of TL-MPA is

$$\hat{a}_u = \begin{cases} 0, & r_u < -15, \\ 1, & \text{otherwise} \end{cases} \tag{15}$$

IV. Data-aided False Alarm Corrector

Based on the redundant factor graph $\mathcal{G}(\hat{\mathcal{U}}_{ac}^I)$, the MPA algorithm [12] can be employed to perform data decoding [5]. The decoding process of the $k^{th}, 1 \le k \le K$ data symbol is formulated as

$$\hat{\mathbf{x}}_u[k] = \mathrm{MPA}(\mathbf{y}[:,k], \mathcal{G}(\hat{\mathcal{U}}_{ac}^I)), u \in \hat{\mathcal{U}}_{ac}^I. \tag{16}$$

However, the existence of the redundant variable nodes in $\mathcal{G}(\hat{\mathcal{U}}_{ac}^I)$ would degrade the decoding performance of MPA. Hence, removing these redundant variable nodes is of great importance, and this motivates our false alarm corrector.

In [8], a symbol energy based false alarm corrector is designed where the false detected users are recognized through detecting the energy of users' decoded symbols. Nevertheless, such a false alarm corrector is susceptible to noise. In this paper, a different false alarm corrector based on multiple zero symbol detection [5] is developed. The key idea is that if a user is active, the detected zero symbol number in its decoded packet $\hat{\mathbf{x}}_u$ should be small, otherwise, the detected zero symbol number should be large. Let $\tau_{zs} \ge 1 \in \mathbf{Z}_+$ denotes the threshold of the detected zero symbol number in any one data

packet of users. For user $u, u \in \hat{\mathcal{U}}_{ac}^{I}$, the proposed false alarm corrector can be summarized as

$$\hat{a}_u = \begin{cases} 0, & K - ||\hat{\mathbf{x}}_u||_0 >= \tau_{zs} \\ 1, & \text{otherwise} \end{cases} \tag{17}$$

where $||\cdot||_0$ denotes the l_0-norm. When $\tau_{zs} = 1$, our false alarm corrector is the same as that in [5]. In practical applications, a smaller τ_{zs} would result in more missing detection, while a bigger τ_{zs} would decrease the performance of the false alarm corrector. In this paper, to balance these two performances, the value of τ_{zs} is chosen as $\lceil \frac{K}{3} \rceil$ empirically, where $\lceil \cdot \rceil$ denotes rounding up to the nearest integer. The pseudo-code of our proposal is given in Algorithm 1.

Algorithm 1 Data aided active user detection

Input: $\mathbf{y}[:,k], k \in [1,K], \mathbf{y}_s$
Output: $\hat{\mathcal{U}}_{ac}^{II}, \hat{\mathbf{x}}_u[k], u \in \hat{\mathcal{U}}_{ac}^{II}, k \in [1,K]$
1: Estimate $\hat{U}_{ac}^{I}$ by MPA detector in (8) - (11) or TL-MPA in (12) - (16); //step 1
2: Construct factor graph $\mathcal{G}(\hat{\mathcal{U}}_{ac}^{I})$;
3: **for** $k = 1 : K$ **do**
4: $\quad \hat{\mathbf{x}}_u[k] = \mathrm{MPA}(\mathbf{y}[:,k], \mathcal{G}(\hat{\mathcal{U}}_{ac}^{I})), u \in \hat{\mathcal{U}}_{ac}^{I}$;
5: **end for**
6: **for** $\forall u \in \hat{\mathcal{U}}_{ac}^{I}$ **do** //step 2
7: $\quad$ **if** $K - ||\hat{\mathbf{x}}_u||_0 \geq \tau_{zs}$ **then** $\hat{a}_u = 0$; $\hat{\mathcal{U}}_{ac}^{I} = \hat{\mathcal{U}}_{ac}^{I} - \{u\}$;
8: $\quad$ **end if**
9: **end for**
10: $\hat{\mathcal{U}}_{ac}^{II} = \hat{\mathcal{U}}_{ac}^{I}$;
11: Construct factor graph $\mathcal{G}(\hat{\mathcal{U}}_{ac}^{II})$;
12: **for** $k = 1 : K$ **do**
13: $\quad \hat{\mathbf{x}}_u[k] = \mathrm{MPA}(\mathbf{y}_k, \mathcal{G}(\hat{\mathcal{U}}_{ac}^{II})), u \in \hat{\mathcal{U}}_{ac}^{II}$;
14: **end for**

V. Complexity analysis

Instead of the perfect factor graph $\mathcal{G}(\mathcal{U}_{ac})$ [2], [3], executing MPA over the factor graph $\mathcal{G}(\hat{\mathcal{U}}_{ac}^{I})$ will not increase the complexity order of MPA in the data decoding part, because the false alarms in $\hat{\mathcal{U}}_{ac}^{I}$ are small. This fact is revealed later in Fig. 2. Hence, we mainly compare the complexity of the AUD part in this section.

The complexity order of OMP and AMP are analyzed in Table I in our previous work [4]. The complexity of DCS is approximately in the same order as OMP. Dominated by (8), the complexity of the MPA based detector $\mathcal{C}_{\mathrm{MPA}}$ is in the order of $\mathcal{O}(L_s 2^{w_r})$. The complexity of TL-MPA can be well approximated by

$$\mathcal{C}_{\mathrm{TL-MPA}} \approx \mathcal{O}(L_s(p_{w_1}\binom{w_1}{w_r} + p_{w_2}\binom{w_2}{w_r})), \tag{18}$$

where $p_{w_1} = 1 - \lfloor \lambda w_r - \lfloor \lambda w_r \rfloor \rfloor$, $w_1 = \lfloor \lambda w_r \rfloor$, $p_{w_2} = 1 - p_{w_1}$, and $w_2 = w_1 + 1$. Finally, the complexity orders of other algorithms are listed in Table I

Table I
Complexity comparison

Algorithm	Complexity order
DCS and OMP in [2], [3]	$\mathcal{O}(N_a L_s N + N_a^3 + N_a L_s)$
AMP in [4]	$\mathcal{O}(L_s N)$
MPA based detector	$\mathcal{O}(L_s 2^{w_r})$
TL-MPA based detector	$\mathcal{O}(L_s(p_{w_1}\binom{w_1}{w_r} + p_{w_2}\binom{w_2}{w_r}))$

VI. Simulation Results and Discussion

In this section, the AUD performance and data decoding performance are simulated. To evaluate the AUD performance, the probability of miss detection (pM) and the probability of false detection (pF) are adopted [4]. To measure the data decoding performance, the symbol error rate (SER) is adopted [13]. The system configuration is given in TABLE II.

Table II
System Configuration

Potential user number N	80
User sparsity λ	0.1, 0.3
Sub-carrier number L_s	39
The value of w_c	2
The value of w_r	4
The packet length K	10
Constellation alphabet size M	2

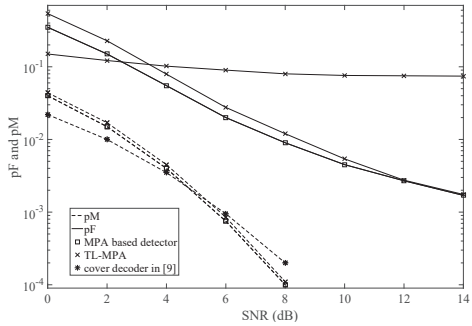

Figure 2. $\hat{\mathcal{U}}_{ac}^{I}$ estimation comparison between the proposed MPA based detector, TL-MPA based detector and cover decoder in [9], where $\lambda = 0.1$.

Firstly, the pF and pM performance of super-set $\hat{\mathcal{U}}_{ac}^{I}$ estimated by the proposed two initial estimators are evaluated. The pF performances of MPA based detector and TL-MPA outperform the cover decoder in [9] significantly when $\mathrm{SNR} > 4$dB. This is because more specific traffic load information ($\hat{\mathbf{Y}}_l$) is exploited by the proposed two initial estimators. Moreover, the performance of TL-MPA is very closed to that of the MPA detector which verifies the efficiency of the proposed TL-MPA scheme.

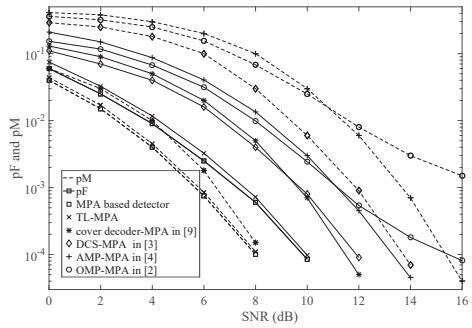

Figure 3. AUD performance comparison between the proposed data aided AUD scheme and its counterparts in [2]–[4], [9] where $\lambda = 0.1$.

The AUD performance of our proposed methods with $\lambda = 0.1$ is shown in Fig. 3. OMP-MPA indicates that the AUD is performed by OMP algorithm and data decoding is performed by MPA represented in (16). In the same spirit, we have AMP-MPA, DCS-MPA. Cover decoder-MPA denotes

that estimating $\hat{\mathcal{U}}_{ac}^{I}$ by cover decoder based on $\hat{\mathbf{Y}}_t$ in (11) and implementing data decoding by MPA. DCS-MPA, which has the best AUD performance in CS based counterparts, has almost the same pF performance as that of the cover decoder-MPA. However, the pM performance of the cover decoder-MPA is significantly better than that of the DCS-MPA. Owing to the higher quality of super-set estimation $\hat{\mathcal{U}}_{ac}^{I}$, the pF performances of the proposed MPA based detector and the TL-MPA based detector outperform cover decoder-MPA significantly.

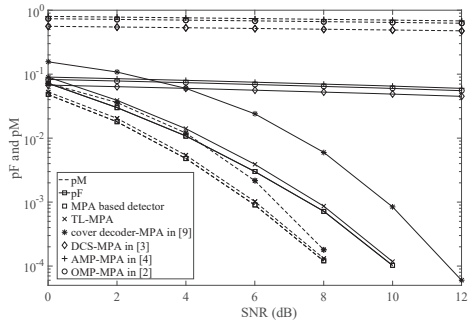

Figure 4. AUD performance comparison between proposed data aided AUD scheme and its counterparts in [2]–[4], [9] where $\lambda = 0.3$.

The AUD performance of our proposed method in a relatively higher user sparsity region, i.e. $\lambda = 0.3$, is shown in Fig. 4. The performance of CS-MPA detectors in [2]–[4] is poor due to the sparsity limitation in CS theory, whereas our proposed methods works well. It implies that more active users can be supported by our methods.

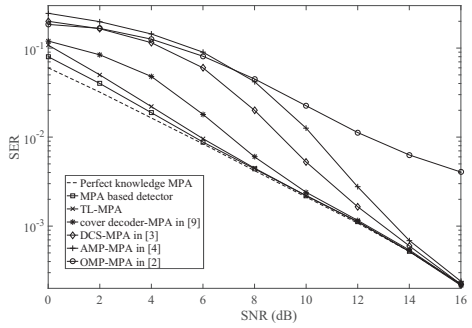

Figure 5. SER performance comparison between proposed data aided AUD scheme and its counterparts in [2]–[4], [9] where $\lambda = 0.1$.

The SER performance of our proposed method with $\lambda = 0.1$ is shown in Fig. 5. The perfect knowledge MPA assumes the active users are all exactly known at the BS, which is the lower bound of our method. Owing to the superior AUD performance represented in Fig. 3, our proposed method achieves the best SER performance.

The SER performance of our proposed method with $\lambda = 0.3$ is shown in Fig. 6. Similar to Fig. 4, it confirms that many more active users can be supported by our method.

VII. Conclusion

In this paper, we transfer the AUD problem as a super-set estimation problem based on the observation that the false detected users could be possibly corrected with the aid

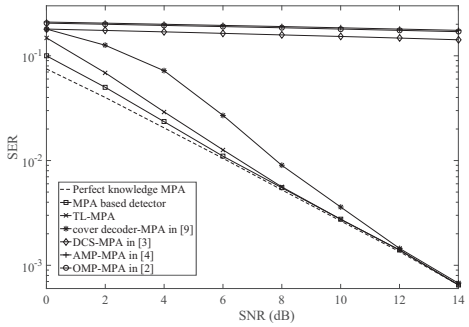

Figure 6. SER performance comparison between proposed data aided AUD scheme and its counterparts in [2]–[4], [9] where $\lambda = 0.3$.

of decoded data symbols. Then, a two-step data-aided AUD scheme with false alarm correction is proposed. To estimate an initial active user set in step 1, the embedded LDS based user preamble pool is constructed and two MPA based initial estimators are developed to realize the detection. In addition, a false alarm corrector is integrated into the data decoding stage to recognize the remaining false detected inactive users in the initial active user set. Simulation results verify the efficiency and superior performance of our proposed methods.

References

[1] M. B. Shahab, R. Abbas, M. Shirvanimoghaddam, and S. J. Johnson, "Grant-free non-orthogonal multiple access for IoT: A survey," *IEEE Communications Surveys & Tutorials*, vol. 22, no. 3, pp. 1805–1838, 2020.

[2] O. O. Oyerinde, "Compressive sensing algorithms for multiuser detection in uplink grant free NOMA systems," in *2019 IEEE 89th Vehicular Technology Conference (VTC2019-Spring)*. IEEE, 2019, pp. 1–6.

[3] B. Wang, L. Dai, Y. Zhang, T. Mir, and J. Li, "Dynamic compressive sensing-based multi-user detection for uplink grant-free NOMA," *IEEE Communications Letters*, vol. 20, no. 11, pp. 2320–2323, 2016.

[4] L. Yang, P. Fan, L. Li, Z. Ding, and L. Hao, "Cross validation aided approximated message passing algorithm for user identification in mMTC," *IEEE Communications Letters*, vol. 25, no. 6, pp. 2077–2081, 2021.

[5] H. Zhu and G. B. Giannakis, "Exploiting sparse user activity in multiuser detection," *IEEE Transactions on Communications*, vol. 59, no. 2, pp. 454–465, 2010.

[6] X. Bian, Y. Mao, and J. Zhang, "Supporting more active users for massive access via data-assisted activity detection," in *ICC 2021-IEEE International Conference on Communications*. IEEE, 2021, pp. 1–6.

[7] J. Van De Beek and B. M. Popovic, "Multiple access with low-density signatures," in *GLOBECOM 2009-2009 IEEE Global Telecommunications Conference*. IEEE, 2009, pp. 1–6.

[8] A. Mazumdar and S. Pal, "Support recovery in universal one-bit compressed sensing," *arXiv preprint arXiv:2107.09091*, 2021.

[9] H. A. Inan, S. Ahn, P. Kairouz, and A. Ozgur, "A group testing approach to random access for short-packet communication," in *2019 IEEE International Symposium on Information Theory (ISIT)*. IEEE, 2019, pp. 96–100.

[10] H. S. Jang, S. M. Kim, H.-S. Park, and D. K. Sung, "An early preamble collision detection scheme based on tagged preambles for cellular m2m random access," *IEEE Transactions on Vehicular Technology*, vol. 66, no. 7, pp. 5974–5984, 2016.

[11] H. Ji, W. Kim, and B. Shim, "Pilot-less sparse vector coding for short packet transmission," *IEEE Wireless Communications Letters*, vol. 8, no. 4, pp. 1036–1039, 2019.

[12] R. Hoshyar, F. P. Wathan, and R. Tafazolli, "Novel low-density signature for synchronous CDMA systems over AWGN channel," *IEEE Transactions on Signal Processing*, vol. 56, no. 4, pp. 1616–1626, 2008.

[13] S. Jiang, X. Yuan, X. Wang, C. Xu, and W. Yu, "Joint user identification, channel estimation, and signal detection for grant-free NOMA," *IEEE Transactions on Wireless Communications*, vol. 19, no. 10, pp. 6960–6976, 2020.